PHILIPP AGRIC SCIENTIST
Vol. 99 No. 1, 68–79
March 2016

ISSN 0031-7454

Net Sediment Transport in Pampanga Bay, Northwestern Manila Bay Derived from Grain Size Trends, Bathymetric Change and Landsat Data

Cherry L. Ringor[1,*] and Fernando P. Siringan[2]

[1]Institute of Environmental Science and Meteorology, University of the Philippines Diliman, Quezon City 1101, Philippines
[2]The Marine Science Institute, University of the Philippines Diliman, Quezon City 1101, Philippines
[*]Author for correspondence; e-mail: cringor@iesm.upd.edu.ph

Pampanga Bay receives 50% of the total annual freshwater budget of Manila Bay and has the largest river sediment input. The supply of high loads of sediments has significant implications on the aquatic productivity, coastal evolution and contaminant dispersal in the bay. Sediment dispersal patterns were determined using Landsat Thematic Mapper (TM) imageries, trends of grain size parameters, and water depth changes. Satellite data showed a west-southwest and southward alongshore transport of suspended sediments. Transport of bottom sediments is defined by the analysis of grain size trends, showing seaward trending vectors in shallow waters (~5 m depths) and landward trending vectors in deeper waters, which indicate that sediments deposited in the offshore region are further reworked predominantly northward toward the middle part of the bay. This transport pattern is further supported by bathymetric changes over a period of 13 yr. The central region of the bay shows net shoaling while deepening is dominant nearshore. Results of this study generally agree with reported numerical circulation models of the bay except near the mouth of the Pampanga River. The differences can be attributed to high rates of subsidence, which were not considered in the models. This study shows that combination of the different methods yields a better understanding of coastal sediment transport since net and seasonal variations in transport pathways can be established as well as the potential of deposited sediments for reworking. Satellite images provide a significant advantage in that they reveal instantaneous lateral distribution and transport of surface sediments, while analyses of grain size trends and bathymetric changes present information on the long-term fate of the sediments after they are deposited over a longer time scale. This multiple approach is particularly useful in the prediction of areas vulnerable to contamination within the bay.

Key Words: bay, bathymetric change, circulation models, grain size trends analysis, Landsat, sediment transport

INTRODUCTION

Pampanga Bay, a sub-basin in the northwestern portion of Manila Bay (Fig. 1), is an important marine environment, both economically and ecologically. It has extensive wetlands with high biological productivity that makes them vital nursery grounds for fisheries. It is the receiving basin of the Pampanga drainage system, the largest watershed draining into Manila Bay which discharges ~119 x 10^5 tons of sediment annually (Japan International Cooperation Agency, JICA unpublished data). The high amounts of sediments being transported in the bay have significant implications on the productivity of aquatic life and coastal evolution.

Suspended sediment is environmentally important from several standpoints. Its entry into suspension may constitute erosional damage, and its deposition may be damaging to channels, harbors and biologically productive wetlands and seafloors. Moreover, sediments act as contaminant traps (e.g., Machado et al. 2008; Feng et al. 2011) and thus play a key role in determining the concentration, distribution and long-term fate of several pollutants in natural bodies. Understanding of the dispersal patterns of the sediment is therefore critical in local and regional coastal planning and management for resource development.

Information on the sediment transport patterns can be obtained directly by such means as aerial photography or remote sensing (e. g., Doxaran et al. 2009; Pavelsky and Smith 2009; Raharimahefa and Kusky 2010), or indirectly by means of sedimentological analyses (e.g., McLaren and Little 1987; Gao and Collins 1992, 1994; Gao et al. 1994; Asselman 1999; Le Roux and Rojas 2007; Ma et al. 2010; Maillet et al. 2011; Sanchez and Carriquiry 2011; Poizot et al. 2013; Zhang et al. 2013; Balsinha et al. 2014), or through coastal circulation modeling (e.g., de las Alas and Sodusta 1985; Villanoy and Martin 1997; Fuji-ie et al. 2002; Fuji-ie and Yanagi 2006; Pokavinich and Nadaoka 2006). The advantage of using remote sensing techniques is that it provides regional interpretation, prediction, and graphical visualization of inaccessible conditions from limited information. It is also cheaper and produces faster assessment of suspended sediment distribution on a frequent basis. However, remote sensing applications only present instantaneous transport of sediment, thus requiring acquisition of high frequency images to sufficiently address temporal variability of coastal processes. Also, remote sensing may only yield information from the uppermost layer of the water column such that the long-term depositional site of the sediments cannot be adequately determined.

Coastal ocean circulation models provide a framework for investigating the basic processes of an evolving coastal ocean, in particular, the transport and dispersal of suspended sediments. They are often dependent upon some information from actual current measurements, which are almost always difficult to obtain due to high cost of instrument and field operation. But similar to remote sensing, it is essential to combine the results from water circulation models with the measured data to provide the best estimates of how water and materials are transported throughout the coastal system (Blumberg et al. 1993). Moreover, data collected by on-site measurements are still necessary for calibration and validation. The bottom sediment record, on the other hand, provides a time-averaged sediment dispersal pattern, which is necessary to integrate all processes responsible for net erosion, transport, and deposition of sediments. By doing sediment analysis, the long-term fate of the sediments can be determined.

This study delineates sediment transport patterns in Pampanga Bay, a shallow embayment in the northwestern part of Manila Bay, Philippines, and the receiving basin of the largest watershed draining into the bay. A key part of this work is the combined use of Landsat, grain size, and bathymetric data in establishing sediment pathways, which permits us to extract and correlate information, both temporally and spatially, from each data set. Although each approach can be used alone, the most holistic and effective approach is the combined use of such data sets. Landsat images provide instantaneous dispersal patterns of suspended sediments before their long-term deposition whereas the grain size trend analysis derived from the upper layers of the bottom sediments gives a time-averaged record that integrate the processes of deposition and possible reworking of sediments. Changes in bathymetry over a few to tens of years provide information on net sediment accumulation which can be used to delineate sediment transport patterns beyond the timescales provided by the Landsat data and grain size trends. Thus, the use of three different approaches gives a more complete picture of sediment movement - from the time the sediment is introduced into the bay to the time when they are reworked after initial deposition. This work also highlights the advantage of using multiple approaches to resolve the limitations of one data set. The results were further compared with existing numerical circulation models in Manila Bay.

The Study Area

Pampanga Bay is a semi-enclosed shallow embayment in the northwestern part of Manila Bay with a basin area of ~450 km^2 (Fig. 1). It is a moderately stratified estuary with a weak halocline at ca. 5 m depth in the water column (Velasquez et al. 2002) and receives more than 50% of the total annual freshwater input into Manila Bay (Environmental Management Bureau, EMB, unpublished data). The main source of sediment and freshwater inflow into the bay is the Pampanga River Basin which discharges ~119 x 10^5 tons of sediment each year (JICA 1982, unpublished). Peak discharge occurs from June to November with maximum discharge of 938 m^3 s^{-1} in August. The river has the lowest discharge during the months of March and April, typically less than 85 m^3 s^{-1} (EMB unpublished data).

The area experiences pronounced wet (June to October) and dry (November to May) monsoon periods with a mean monthly rainfall of ~86 mm averaged from 1969 to 1997 (Philippine Atmospheric Geophysical and Astronomical Services Administration, PAGASA unpublished data). The average monthly rainfall during the wet season is ~173 mm which drops to ~25 mm during the dry months. The driest month is January with an average rainfall of only 4 mm and August is the wettest month when mean precipitation reaches up to 252 mm.

Although tropical cyclones can occur at any time of the year, the majority of those that threaten Manila occur from June to December with July having the highest frequency (PAGASA unpublished data). Despite the frequent occurrence of storms, an average of more than four each year, topographic features surrounding Manila Bay help shelter the bay from severe winds. At least three major wind regimes dominate the bay. Northeasterly winds with speeds averaging ~5 m s^{-1} prevail from October to January; southeasterly winds with speeds ranging from 3 to 6 m s^{-1} are dominant from February to May; and southwesterly winds with speeds of 5 to 7 m s^{-1} dominate from June to September (de las Alas and Sodusta 1985). The dominant wind is toward northwest-northeast.

The bottom of Pampanga Bay is rather featureless with an average depth of ~7.5 m and reaches a maximum of ~20 m (Fig. 1). Sea floor gradients are gentlest, 1:3500, from the farthest northwestern coast of Pampanga Bay out to a depth of 3 m, while along the southwest coast out to ~12 km offshore, the bathymetry of the bay is a lot steeper with a slope of 1:200.

The watershed of Pampanga Bay is primarily agricultural, of which 3.35 km^2 of land is cultivated for rice and diversified crop production (National Water Resources Council, NWRC unpublished data). The coastal plain is a wide, low-lying surface of a tidal-river delta plain as indicated by a mosaic of branching tributaries and meandering tidal channels. The landward limits of nipa palms and fishponds indicate northward tidal incursion of more than 20 km into the northwestern delta plain (Siringan and Ringor 1997). Tides are primarily diurnal and within the microtidal range. The estimated diurnal tidal range at the mouth of the Pampanga River is 0.95 m and a mean tide level of 0.44 m is reckoned from the mean lower low water (National

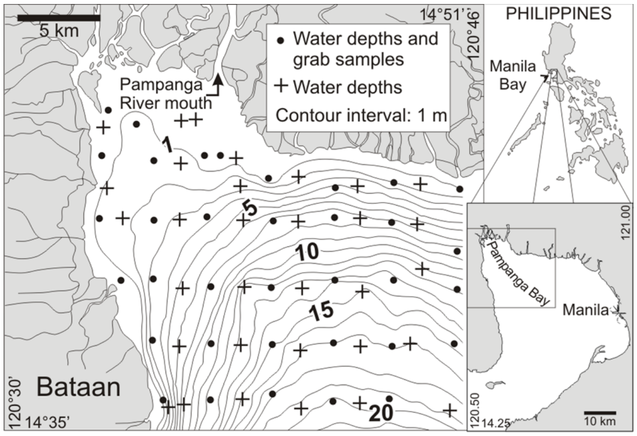

Fig. 1. Location of the study area and samples collected. Also shown is the 1998 bathymetry of Pampanga Bay (reduced to the approximate level of mean lower low water). Black dots mean both samples and water depths were taken; crosses mean only water depths were taken.

Mapping and Resource Information Authority, NAMRIA, unpublished data).

Wave height along the coast of Manila ranges from 0.76 to 1.7 m, with an average of 1.27 m. The mean wavelength is ~47 m with a wave period ranging from 5 to 6.5 s (Salzgitten Consult GmBH unpublished data). However, waves characterized with such periods may have been intensified by the interaction of stronger waves from the South China Sea where the average wave period is estimated to be 5–6 s based on wind wave parameters (Sui 1994). Calculation of wave period (after Thurman 1988) based on the average wind speed of Manila Bay, 5 m s^{-1}, yields a lower value of ~3.9 s. The waves generated by typhoons could reach 3 m or more in significant height due to the shallow bottom, but should not build to excessively high levels (Naval Environmental Prediction Research Facility unpublished data).

MATERIALS AND METHODS

Field Data

Thirty-five seabed sediment samples were acquired for grain size analysis on ~4 km-grid intervals (Fig. 1; Table 1) using a Ponar-type grab sampler. Grid sampling was done to analyze suitable trends or patterns that may indicate possible reworking of bottom sediments using a sediment transport model developed by McLaren and Little (1987) and later adapted by Gao and Collins (1992). The upper 10–20 cm of the sediment column was sampled since the study is concerned with the net sediment transport direction. It is assumed that what was sampled constitutes the average of all the transport processes affecting the sample site.

Spot measurements (n=67) of water depths (Fig. 1) were made using a single beam echo sounder, with a resolution of 30 cm, to update the bathymetric chart of the bay. The average spacing of soundings along the survey lines was ~2 km, comparable to the data points of the 1985 nautical chart used to calculate the bathymetric change. The survey was run along a pre-planned boxed grid at 4 km-spacing extending roughly 20 km alongshore and 16 km offshore, to ~20 m water depths. The total area covered by the survey is ~450 km^2 and ~15 depth measurements were taken every 100 km^2. The locations of the stations were determined using a hand-held GPS (±10 m accuracy). Fieldwork was done during the dry NE monsoon months of February and May in 1998.

Delineation of Suspended Sediment Transport using Landsat Images

The Landsat images were used to identify the source and delineate the direction of the suspended sediment flow on the surface water. Transport of suspended sediments was determined by tracing tonal variations of the turbidity plumes that define the flow direction of the plumes. Analog records of Landsat Thematic Mapper (TM) images taken on December 3, 1989; February 19, 1995; and March 25, 1996 were analyzed. Finley and Baumgardner (1980) have suggested that the wind pattern over a period of time prior to the image date must be considered in analyzing the observed phenomenon. In their work, the average wind velocities and direction 3 d before and after the image date were considered. For this study, wind data 3 d prior to the data acquisition were taken into account. The 3-d winds represent the sustained winds, which are thought to affect the subtidal shelf-estuarine exchange and contribute momentum to inner shelf currents (Wiseman et al. 1988). The suspended sediment concentration was not estimated since the study was interested in the surface sediment movement.

Comparison of Landsat data with modeled circulation of Manila Bay from previous studies was also done to qualitatively compare observations of suspended sediment flow patterns. However, modeled current patterns for only two wind regimes, northeast and southeast winds, were compared with the satellite data since no Landsat image was obtained during occurrence of the southwesterlies. Also, in the absence of a circulation model for north winds, it is assumed that north winds will produce a pattern very similar to that of northeast winds. Thus, the December 3, 1989 image acquired during the northerlies was compared with the northeast circulation model.

Grain Size Analysis of Surface Sediment Samples

Approximately 30 g of homogenized sediment was taken in each sample for analysis of grain size fractions. Each sub-sample was desalinized to remove quantities of salt within their interstitial waters that may cause flocculation of sediment particles although it has been reported that flocculation does not seem to have any negative effects on the applicability of grain size trends for sediments with mean sizes ranging from 3.53 to 7.31 Φ (Asselman 1999). The samples were separated into sand (−1 to 4 Φ) and mud (> 4 Φ) fractions by wet sieving method. The mud fraction was further analyzed using the pipette method at 1 Φ interval (from 4–8 Φ), described by Lewis

Table 1. Location of the samples and their sedimentological parameters.

Sample ID	Location		Grain Size (%)			Moments Measure (phi)		
			%Sand	% Silt	%Clay	Mean	Sorting	Skewness
1	14.733	120.782	1.40	84.98	13.60	5.425	1.466	1.237
2	14.718	120.753	2.40	60.74	36.80	6.913	1.535	-0.462
3	14.733	120.718	2.50	65.47	32.10	6.788	1.514	-0.317
4	14.734	120.683	1.50	62.24	36.30	6.813	1.603	-0.355
5	14.734	120.653	1.80	62.25	36.00	6.868	1.548	-0.400
6	14.736	120.616	2.40	67.98	29.60	6.546	1.613	-0.100
7	14.733	120.584	4.20	63.61	32.20	6.724	1.554	-0.295
8	14.734	120.556	14.60	64.21	21.20	5.812	1.787	0.368
9	14.767	120.557	4.80	73.99	21.20	5.890	1.688	0.495
10	14.793	120.558	3.70	76.91	19.40	5.941	1.620	0.459
11	14.751	120.755	65.30	28.50	6.20	4.299	1.406	1.910
12	14.755	120.718	36.90	50.16	12.90	5.003	1.727	1.027
13	14.752	120.684	8.60	66.40	25.00	6.069	1.764	0.222
14	14.754	120.650	35.20	53.57	11.20	4.931	1.634	1.151
15	14.762	120.584	2.80	66.07	31.10	6.767	1.546	-0.376
16	14.784	120.574	2.10	59.47	38.50	7.080	1.478	-0.668
17	14.767	120.611	1.40	83.19	15.40	5.839	1.428	0.764
18	14.702	120.751	5.40	61.05	33.60	6.558	1.742	-0.223
19	14.701	120.718	5.30	61.60	33.10	6.658	1.670	-0.321
20	14.700	120.685	4.00	58.39	37.60	6.764	1.687	-0.389
21	14.695	120.650	2.30	52.05	45.70	7.077	1.615	-0.680
22	14.698	120.618	1.30	55.15	43.50	7.039	1.582	-0.604
23	14.701	120.586	1.40	75.46	23.20	6.058	1.659	0.410
24	14.699	120.568	32.40	56.29	11.30	4.873	1.596	1.349
25	14.669	120.585	0.70	95.72	3.60	4.727	0.861	3.641
26	14.664	120.617	0.70	67.21	32.10	6.858	1.445	-0.293
27	14.664	120.750	1.60	63.82	34.60	6.836	1.495	-0.262
28	14.665	120.718	1.50	71.74	26.80	6.598	1.406	0.145
29	14.666	120.684	6.90	65.45	27.70	6.373	1.697	-0.116
30	14.663	120.651	0.80	60.80	38.40	6.912	1.530	-0.366
31	14.634	120.593	10.10	67.48	22.40	6.007	1.724	0.249
32	14.638	120.617	1.00	71.45	27.60	6.349	1.634	0.160
33	14.640	120.650	1.20	70.31	28.50	6.598	1.538	-0.093
34	14.637	120.684	1.50	74.08	24.40	6.337	1.591	0.143
35	14.636	120.716	1.80	61.66	36.60	6.774	1.625	-0.302

and McConchie (1994). Although two methods were used to determine the grain sizes, Le Roux and Rojas. (2007) reported that the particular method used to determine the grain size distribution and parameters does not seem to be too important, as the relative values between sampling points are more important than the absolute values. Weight percentages for each sand, silt and clay component were calculated to generate sediment distribution maps. The grain size data were further used to compute the mean grain size, sorting coefficient and skewness for each sample using the formulae described by Folk and Ward (1957). The granulometric parameters derived served as inputs in the delineation of net sediment transport paths using the method of Gao and Collins (1992) and Gao et al. (1994).

Determination of Net Sediment Transport Based on Grain Size Trend Analysis

Grain size trend analysis is based upon the assumption that the trend used for the analysis has a significantly higher probability of occurrence in the direction of net transport than in other directions. Employing the three most frequently used grain size parameters (mean grain size, sorting coefficient, and skewness), Gao and Collins (1992) and Gao et al. (1994) identified two grain size trends which have higher probability of occurrence in the direction of net transport. Assuming that the net transport is from site A to B, the grain size trends are:

1 $M_A \geq M_B$, $S_A \geq S_B$, $Sk_A \leq Sk_B$
2 $M_A \leq M_B$, $S_A \geq S_B$, $Sk_A \geq Sk_B$

where M is mean, S is sorting and Sk is skewness. These trends have been examined by comparing them with known sediment transport pathways based on current meter measurements and bedform surveys in an inner continental shelf (Gao et al. 1994). Results of these studies indicate that the combination of types 1 and 2 trends showed a relatively high degree of similarity to the identified pathways. Subsequently, such a combined trend has been used in a number of investigations, producing patterns consistent with those defined by artificial tracer experiments or transport formulae using measured hydrodynamic data (Ma et al. 2010; Sanchez and Carriquiry 2011) and known oceanographic drivers for the external shelf and measured near-bottom currents (Balsinha et al. 2014). Even with such validations, however, Le Roux and Rojas (2007) pointed out that different trend types (other than 1 and 2) produced different results, which are all statistically valid and that a particular trend type produced statistically significant results for specific sedimentary environment. This means that the choice of trend type must be based on either a thorough understanding of the depositional and transport processes or on additional information on likely sediment transport paths. Hence, it was first assumed that the particular trend type used in this study (i.e., combination of types 1 and 2 trends after Gao et al. 1994) would produce a bottom sediment transport pattern commonly observed in an estuarine environment. Since the initial results are generally consistent with the depositional and transport processes in an estuary and supported by bathymetric change data, other trend types were not further analyzed and compared. The analytical procedures for determining the trends were adopted from Gao and Collins (1992) and Gao et al. (1994).

For this work, the magnitude of transport vectors is not considered, only the direction, and it is assumed that the sediment samples are a product of the same depositional event reflective of time-scale recorded by the sampled sediment. Radiomateric dating of the sediments west of the study area estimated a sedimentation rate of 5.5. cm/yr (Santos and Villamater 1986), which indicates that the 10–20 cm sampling depth represents a depositional time of ~1.8–3.6 yr (medium-term). A characteristic distance, which is the maximum spatial sediment sampling interval, of 4 km was used. To determine whether or not a spatial relationship exists between the sample sites at such a distance, geostatistical analysis using spherical semivariogram modeling was done. Filtering (or averaging) operation was also applied to remove noise or vectors that are not in agreement with the general pattern. Here, it is assumed that the various components of noise do not show any ordered pattern: when observed in a frequency domain, these components are present in the form of high frequency fluctuations. Although Asselman (1999) and Le Roux et al. (2002) showed that filtering reduces the spatial resolution and produces trends from completely random data, a recent work by Le Roux and Rojas (2007) demonstrated that smoothing the data using a technique similar to that employed in the Gao and Collins method, produced statistically valid trends from some trend types. They recommended that smoothing of the original vectors can be done once their statistical validity has been established as this can produce trends that do not actually exist in nature. Since our results generally describe the dynamics of sediment movement in estuaries and are consistent with the results of the bathymetric change data, we removed the noise by averaging the vectors of a particular sampling site with those at adjoining sites. The length of the vector is assumed, for convenience, to be unity because the mean, sorting and skewness all combine to form a trend, hence, it is difficult to define the length of the vector on the basis of the parameters themselves without any bias toward one of the parameters. The net transport maps were generated using a BASIC program.

Assumptions in the Grain Size Trend Analysis

The grain size trend analysis works best in sandy sediments due to the effects of flocculation. Stevens et al. (1996) reported that fine silt and clay have limited sorting due to their deposition from aggregated suspension and their characteristics are inherited from the sediment source, not necessarily from transport processes. They suggested that the fine-silt and clay fractions be evaluated separately and used in conjunction with mineralogic, geochemical or biological parameters. Also, the interpretation of transport vectors can be improved if sub-environments (in relation to sedimentological processes) in the study area have been identified. Still, a few studies have applied the grain size trends analysis to fine sediments. For example, Zhang et al. (2013) used the Gao and Collins method on the clayey silt and silty clay sediments of the Pearl River Estuary and the result is consistent with the residual current circulation pattern. The method was also used by Cheng et al. (2004) to determine net sediment transport patterns in Bohai Strait where the dominant grain sizes of the bottom sediments are silt-clay silt. Their result is consistent with current circulation pattern in the area and the interpretation of strata from seismic reflection data. Another study by Duman et al. (2004) in Izmir Bay, western Turkey also applied grain size trend analysis to sandy silt-silt sediments. In this study, it is assumed that size sorting of fine-grained sediments can still occur when subjected to bottom shear stresses (Law et al. 2008). Also, as further discussed below, the grain size trend analysis assumes the integration of all processes responsible for transport and deposition at the sampling site which may involve resuspension and or reworking. However, for a more accurate depiction of bottom sediment transport, it is recommended that other data from hydrodynamic, mineralogical, or geochemical investigations be used in conjunction with grain size.

There are also several considerations regarding the determination of the characteristic distance. Spatial correlation between the sampling sites is commonly determined using semivariogram modeling since at very wide sample spacing, there may not even be any correlation between the samples (Stevens et al. 1996). However, as reviewed by Kairyte and Stevens (2015), the semivariogram models should not be overinterpreted since there are several variables to consider and suggested further evaluation using population anomalies if the reliability of values in individual raster cell is low. McLaren et al. (2007) reported that transport processes could be reliably detected over a distance twice or more of that of the sampling distance. Less than this, the trend vectors may record noises or create spurious transport pathways through the processes of “aliasing”. Ultimately, McLaren et al. (2007) suggested considering the number of sedimentological environments, the desired spatial scale of the sediment trends, and the extent of the study area when selecting suitable sample spacing. Our study area is a small sub-basin of Manila Bay, which can be regarded as one specific site or type of environment as opposed to the entire Manila Bay where the hydrodynamics is not uniform throughout and contains sub-environments.

It is also assumed that the grain size trend does not only represent one transport process and does not have any direct time connotation (McLaren et al. 2007) but an integration of all the processes responsible for transport and deposition (a review can be found in Kairyte and Stevens 2015). The method is used to analyze if there is a sediment transport relationship between the neighboring deposits. In the study area, estimates of radionuclide-derived sedimentation rate give a value of 5.5. cm/yr (Santos and Villamater 1986), which indicates that the 10 –20 cm sampling depth represents a depositional time of ~1.8–3.6 yr.

Recent work of Kairyte and Stevens (2015) shows that a combined method for interpreting transport pathways using the grain size trends in the Lithuanian coast provides more complementary information about the sedimentary environment. They used population statistics to identify overall erosional and depositional sites in conjunction with transport vectors for site-specific interpretations. Indeed, the use of grain size trend analysis for sediment transport studies can still be improved. However, if the overall transport trend is realistic to the environment and is corroborated by other data set, the method used in this study could still be helpful. In the case of the present work, the transport pattern is reflective of an estuarine environment, which is the study area. Also, the grain size result complements the long-term sediment accumulation derived from the bathymetric data. Moreover, the goal of this study is not only focused on the grain size trend analysis method. We wanted to show the transport of suspended and bottom sediment from the source to its long-term depositional sites at different time scales using the combined information from Landsat (instantaneous), grain size (medium-term), and bathymetric change (long-term). With the recent availability and accessibility of Landsat images and high resolution echo sounders, we believe that the combined approaches can be more useful. But the information will not be complete without insights from the grain size trend analysis.

Determination of Bathymetric Changes

Changes in water depth were determined for identification of zones of bottom sediment accumulation and erosion on a longer time scale. Calculation of bathymetric changes using the newly acquired hydrographic data was done by plotting the tide-corrected 1998 depths on the 1985 bathymetric chart and subtracting the depth values at individual points. The resulting difference was contoured at an interval of 0.5 m (see Results, Fig. 6).

RESULTS

Spatial Distribution and Transport Directions of Suspended Sediments Derived from Landsat TM Data

The December 3, 1989 satellite image shows suspended sediment entering the bay area from the northern coast (Fig. 2a). Plume coming out of the Pampanga River extended for a distance of ~10 km from the river mouth reaching out to water depths of 5 m. The dispersion direction is veered slightly to the southwest. Off the Labangan Channel, the plume disperses radially and can be traced out to extend over the water depths of 7 m. In general, the plumes appear to extend southward of the Pampanga Bay following the predominant wind direction with speeds of 3–5 m s^{-1} during the period. The size and the tonal characteristics of the plumes, compared with the other images used, indicate a relative low discharge event (Fig. 2a–c).

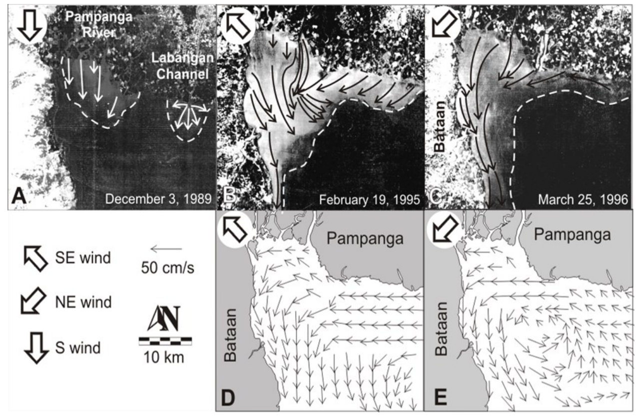

Fig. 2. Comparison of Landsat data (A–C) with circulation models of Manila Bay (D–E). For the December 3, 1989 image (A), the prevailing northerly winds are assumed to produce a circulation pattern very similar to the NE winds. Dashed lines denote the extent of the sediment plume. Large arrows indicate wind direction. Circulation models were modified from de las Alas and Sodusta (1985).

On February 19, 1995, rivers have higher discharge as clearly shown by increased turbidity and extent of plume dispersion in the Landsat image (Fig. 2b). All the major rivers have associated extensive sediment plumes, which converge offshore, resulting in a major plume veered slightly to the southeast. Near the coast, concentration of suspended matter is also observed, except in the northwesternmost part of the embayment where a reduction in turbidity is seen. The dispersion of suspended sediments observed from the satellite image suggests a counterclockwise flow direction. Near the margins of the northern coast, the image shows westward veering of surface waters which seem to follow the 2–5 m isobaths, while along the western coast, sediments move generally southward where plumes are seen fringing the coast. During this period, the area is dominated with relatively weaker (3 m s^{-1}) southwest winds.

Landsat data taken on March 25, 1996 showed lower river discharge than the previous period (Fig. 2c). The prevailing wind direction is northeast with speeds of 3–4 m s^{-1}. Along the northeastern coast, only very slight turbid waters were seen fringing the shore. The plume drifted southwest and converged with the Pampanga River plume before flowing southward parallel along the Bataan shore. Zones of high turbidity were found near the margins of the bay, particularly near the river mouths. The dispersion of plumes showed an elongate pattern drifting parallel to the shoreline. The prevailing path of sediment plumes followed the same transport direction delineated in the February 19, 1995 data, which showed a counterclockwise flow of turbid waters. Overall, the offshore turbidity patterns, captured by Landsat imageries from three different periods, showed a west-southwest suspended sediment transport direction off the Pampanga coast and a southward alongshore transport off the Bataan coast (Fig. 2a–c).

Distribution and Transport Directions of Bottom Sediments Derived from Grain Size Trend Analysis

Most of the bay's substrate was clay silt with fractions of silt-silty sands concentrated near the shore (Table 1; Fig. 3a–d). Clays generally increased in abundance toward the central region of the bay (Fig. 3a). High amounts of sand were dominant near the mouths of rivers (Fig. 3c).

Poorly sorted sediments with a mean grain size of 6.5–7.0 Φ dominated the bay (Table 1; Fig. 3e). In general, sorting coefficients gradually improved from the center of the embayment toward the coast. Northwest of the bay, fine-grained sediments showed relatively lower sorting coefficients. Skewness was dominated by positive values near the shore (Fig. 3f). Negative values, which are dominant in the interior of the embayment, are generally associated with samples of relatively high sorting coefficients.

The semivariogram model indicates that the sill is reached at ~5.5 km which means that a spatial correlation still exists between the samples (Fig. 4). Net transport patterns derived from the grain size trends showed transport vectors pointing southward along the margins of Pampanga coast (Fig. 5). Off the northern Bataan coast, east-southeast trending vectors are dominant; in the south, they are directed to the north-northeast. Southeast of the bay, the trends are mainly toward the northwest. The vectors converge in the middle part of the bay. In general, two distinct patterns of transport vectors can be delineated: seaward trending vectors in shallow waters (~5 m depths) and landward trending vectors in deeper waters.

Net Sediment Accumulation (13 yr) Derived from Water Depth Changes

The 1998 bathymetry derived from the water depth data shows a northwest-southeast landward extending isopleth that forms over a broad and shallow shelf in the northwestern region of the bay (Fig. 1). Water depths in this area range from <1 to 2 m and gradually deepen to the southeast up to depths of 20 m. Gently sloping shelf gradient also characterize the northeastern part of the bay and becomes steeper and narrower in the southwest (Fig. 6). Contours parallel the northeast and southwest shoreline from a depth of 2 m.

Between the period of 1985 and 1998, depths in most of Pampanga Bay have decreased markedly, with an average of ~1.3 m (Fig. 6). The central region of the bay displays high values of shoaling, where as much as 3.1 m of shoaling was recorded. In shallower waters, at depths of 1–4 m, deepening is dominant. The patterns of shoaling and deepening indicate that areas near the shore

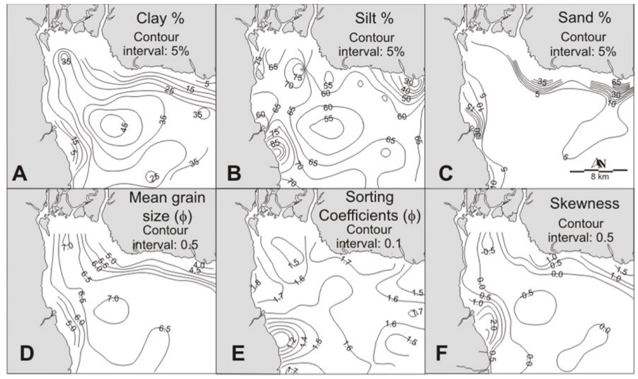

Fig. 3. Distribution patterns of sediment sizes (A–C), mean grain size (D), sorting coefficient (E), and skewness (F). The central region of the bay is dominated with clay while sands are abundant near the mouths of major rivers.

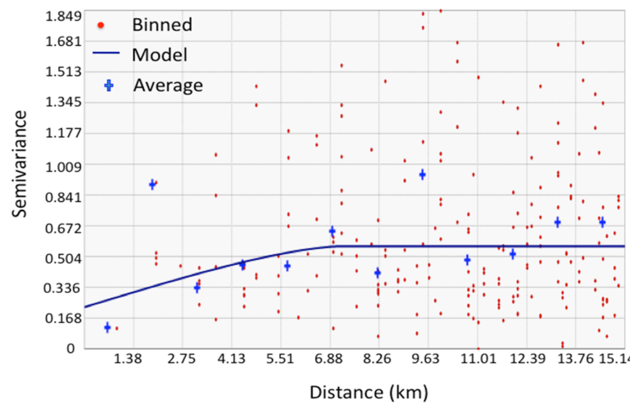

Fig. 4. Omnidirectional semivariogram model using sediment mean values indicates that the sill is reached at ~5.5 km.

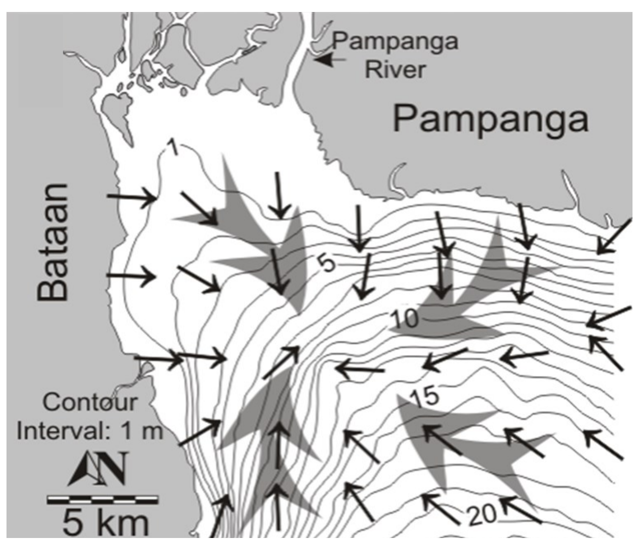

Fig. 5. Net sediment transport patterns from the combined grain size trends 1 and 2. The transport patterns show convergence of vectors in the central part of the embayment. Also shown is the bathymetry. Sediment transport model after the method of Gao et al. (1994).

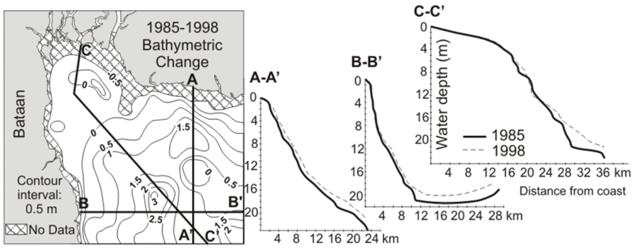

Fig. 6. Bathymetric changes (± 0.30 m accuracy) between 1985 and 1998. Comparison of the seafloor gradients show a general shallowing toward the offshore region of the bay.

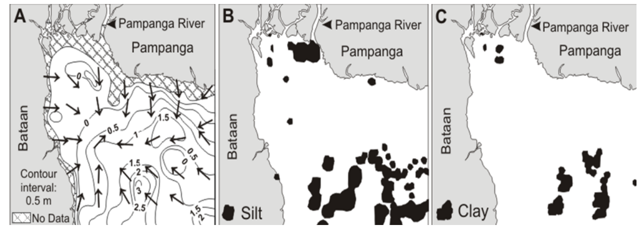

Fig. 7. Bathymetric change (1985–1998) map superimposed with net bottom sediment transport from grain size analysis (A). Net horizontal distributions of deposited silt (B) and clay (C) from numerical modeling (modified from Fuji-ie and Yanagi 2006).

are zones of deepening while the central regions of the bay are sinks. Highest value of deepening is ~1 m with an average of ~0.4 m. Northeast of the bay, shoaling of as much as 1.5 m occurred.

Comparison of the seafloor depths delineated from the bottom profiles clearly show shoaling in 1998 as indicated by the gentler shelf relative to 1985 (Fig. 6). Profile perpendicular to the Bataan coast shows that major shoaling occurred ~10 km from the shore at water depths of 19 m while deepening is apparent out to a distance of 2 km from the coast. In profile A-A', deepening also occurred ~3 km from the shore; shoaling is dominant in the offshore region.

DISCUSSION

Net Sediment Transport Patterns

Offshore turbidity patterns captured by Landsat imageries from three different periods show a west-southwest suspended sediment transport direction off the Pampanga coast and a southward alongshore transport off the Bataan coast. Bottom sediments, which were deposited either by particle settling in the water column or by direct river input, were transported toward the central region of the bay. This pattern of bottom sediment transport as depicted by the grain size trends is supported by the longer-term record (13 yr) of bathymetric change (Fig. 7a). The data clearly shows that deepening is more dominant near the coast while higher accumulation of sediment is evident toward the central portion of the bay.

The net sediment transport pathways in Pampanga Bay demonstrate the patterns of sediment movement and deposition active in coastal plain estuaries: a two-layer circulation with net seaward motion in a surface layer and net landward flow in a bottom layer (Goodrich and Blumberg 1991). During floods, large river outflows may have enough momentum to drive the whole water column off the river mouths to move along the same direction. Under these conditions, sediment-laden waters are pushed through very gently sloping shelf of the bay until it reaches the deeper waters where there is a marked transition between fresh and salt water. At this point, particulate materials are being precipitated out of suspension by salt flocculation and sediments start to accumulate. During low discharge events, the water column becomes nearly vertically homogeneous as there is less influx of freshwater into the bay, hence, tidal exchange combined with high velocity north-bound wind-generated currents may be responsible for the observed onshore reworking of bottom sediments.

Shoaling waves in the Pampanga Bay may also have a major role in the onshore reworking of sediments. Wave heights of ~0.33 m are sufficient to move fine sand in 6–8 m of water (Fleischer et al. 1977). Along the coast of Manila, wave height ranges from 0.76 to 1.7 m (Salzgitten Consult GmBH unpublished data), indicating that waves in the area may transport sediments even at water depths below 8 m. However, reworking of sediments landward is probably more related to flood-tide generated currents. A possible indication that flood-tide generated currents strongly influence the seafloor is the common occurrence of *Nipa fruticans* along the northern coastal plain of the bay (Siringan and Ringor 1997). The brackish environment and the salinity profile data also indicate that salt-water wedge intrusions are occurring along the coastal plain. The very gentle gradient in the northwestern part of the bay may also be amplifying the effect of the ~1 m tidal range. Although the tide range is small, the large bay area allows development of large tidal prism resulting in an increased volume of tidal inflow and the load of bottom sediments it carries. A study done by Horn and Mason (1994) also shows that more sediments, particularly bottom sediments, were transported during the flood phase of high tide than on the ebb.

The dominant shoaling offshore and apparent deepening nearshore might also be due to the efficient flushing of sediments toward the deeper waters. At high river flow, the center mass of the turbidity maximum has been pushed downstream, and the concentration gradients are relatively less steep (Dyer 1994). Hence, there is a possibility of greater loss of material from the estuary into the bay waters, such that lesser volume of sediments is transported back nearshore relative to what is transported offshore. Also, reworking of sediments may have occurred only on the upper surface of the bottom sediments where the grab samples were collected. Another contributing factor, which would decrease the amount of shoaling near the coast, is subsidence as suggested by Siringan and Ringor (1998).

Results generated from the satellite images, trends of grain size parameters, and bathymetric changes provide an overall scenario of the transport and long-term fate of sediments once they enter the bay. Landsat data, which are limited to detection of surface properties of the water column, display the actual pattern and transport mode of suspended sediment load. Analysis of the grain size trends can be used to define net transport pathways of bottom sediments. Bathymetric changes present sediment transport and accumulation within the bay in a longer time span.

Comparison with Numerical Circulation Models of Manila Bay

Suspended Sediments

Aside from providing depositional areas of sediments, the prevailing coastal currents and wind directions can also be inferred by examining the spatial and temporal distribution patterns of suspended sediments derived from satellite images. This information is useful in developing and validating predictive models of circulation patterns. Thus, the suspended sediment flow patterns derived from the Landsat data were correlated with the wind-driven circulation models of de alas Alas and Sodusta (1985). Although the flow of suspended sediments along the Bataan coast derived from the satellite data is generally in good agreement with the circulation models of de las Alas and Sodusta (1985), significant differences were observed in areas near the Pampanga coast. Modeled circulation for northeast and southeast winds predicts a westward veering flow of surface sediments along the whole length of Pampanga coast (Fig. 2d–e). On the other hand, the Landsat image acquired during northerly winds (December 3, 1989) show a predominant southward dispersal pattern of sediment plumes. The same southward transport near the Pampanga coast is also observed in the images obtained during northeast (March 25, 1996) and southeast (Feb. 19, 1995) winds, except in the northeastern and southwestern parts of the bay where it follows the flow of surface waters predicted in the models. Differences between the actual and predicted transport, particularly in areas near the northern coast, may be due to the effect of freshwater discharges into the bay, which was not considered in the models. The modeling done by de las Alas and Sodusta (1985) simulates the response of the bay to the quasi-steady forcing of the prevailing wind only. The influx of large volume of suspended sediments, especially in very shallow regions near the source, may mask the influence of wind and tidal currents in transporting the sediments. Large river outflows may push circulation patterns completely out of the river mouths so that the water moves predominantly seaward. Under these conditions, most of the inflowing river sediments would be carried directly out of the bay. Likewise, the modeled circulation is depth-integrated, velocity and direction-wise thus, they may not necessarily reflect surface water movements highly influenced by large river discharge.

Bottom Sediment

Fuji-ie and Yanagi (2006) used a three-dimensional numerical model, which includes tidal current, residual flow, and current due to wind waves to investigate the sedimentation process of suspended matter in Manila Bay. Their calculated horizontal distribution of deposited silt shows higher accumulation in the deeper, central parts of Pampanga Bay (Fig. 7b and c). This pattern of sediment deposition supports the net transport patterns depicted by the grain size analysis and bathymetric change (Fig. 7a) in the present study except near the mouth of the Pampanga River. The difference can be attributed to the occurrence of subsidence in the area, which was not considered in the numerical modeling and the lack of water depth data. The calculated residual currents from the model show the generation of a clockwise gyre from June to September which reverses to counterclockwise rotation from November to January at depths of ~10 m in the Pampanga Bay area. The formation of gyres may have prevented further transport of sediments, thus sediments tend to be deposited in the deeper central region of the bay.

A similar study by Pokavinich and Nadaoka (2006) simulates the hydrodynamics of Manila Bay using three-dimensional turbulent flow model that took into account the influence of tide, salinity, solar radiation, and wind. Their model suggests greatest contribution of salinity to the bay's circulation for both the upper and lower layers, with weaker vectors in the lower layer. In the upper layers, velocity fields point to south-southeast toward the bay mouth while in the lower layer, they are directed northward toward the coastal margins. The lower layer vectors also become weaker as they reach the coast. This pattern of circulation also reflects the onshore reworking and transport of bottom sediments indicated by the grain size trends.

Implications of Onshore Sediment Transport on Residence Times and Reworking of Pollutants

Wastes derived from fertilizers and insecticides used in farm cultivation combined with waste spills of potentially toxic substances from coastal commerce along the coast of Pampanga Bay are just a few of the sources of pollutants in the bay. The sediment-derived onshore dispersal patterns indicate that once the sediments are deposited, other transport processes further reworked them. Bottom current velocities greater than 15 cm^{-s}, when aided by bioturbation, are sufficient to erode cohesive clay beds (Singer and Anderson 1984). Bottom sediments within the bay have water content of ~80% which can be easily eroded or reworked, suggesting that a current velocity of ~10 cm^{-s} is sufficient to erode the sediments. Wind-induced current velocities in the bay are ~10 cm^{-s} (Villanoy and Martin 1997) which is strong enough to influence reworking of sediments.

The net onshore transport of reworked sediments may imply a larger residence time of pollutant-laden sediments in the coastal waters. A study of nutrient and water budget in Manila Bay shows that the total exchange (flushing) time of the bay waters is 0.09 yr or

~1 mo (Jacinto et al. 1999). Although the estimate is based on waters, very fine unconsolidated sediments, which are easily reworked by coastal currents can also be washed out of the bay. However, the onshore reworking of sediments, which may contain contaminants, may increase their residence times.

CONCLUSION

Offshore sediment transport and dispersal patterns in the Pampanga Bay region were derived through analyses of Landsat TM imageries, grain size trends, and water depth changes. The satellite images showed a west-southwest and southward alongshore transport of suspended sediments, while analysis of grain size trends indicated that sediments deposited in the offshore, deeper parts of the bay were further reworked predominantly northward toward the central part of the bay. Bathymetric changes demonstrate sedimentation in the bay for a period of 13 yr, where net shoaling and general deepening nearshore was observed. This trend is despite the high influx of river sediments into the bay. The possible scenario of sediment transport in the bay can be summarized as follows: during high discharge events, sediment-laden waters are pushed through very gently sloping shelf of the bay until it reaches the deeper, calmer waters where deposition occurs. During low discharge events, sediments are reworked onshore which is mainly attributed to the characteristic circulation patterns in estuarine environments and the interaction with wave-, wind-, and flood-tidal currents. However, lesser volumes of sediments are transported back nearshore relative to what is transported back offshore. In addition, subsidence may mask the effects of deposition, hence, the apparent deepening near the coastal margins. The results of this study are in general agreement with the reported circulation models of Manila Bay except near the mouth of the Pampanga River.

The pattern of net sediment transport has significant implications on the possible distribution of contaminants in the bay. Offshore transport of suspended sediments shown by Landsat images does not necessarily mean that sediments will follow the same transport pathways once they are deposited. Grain size analysis of bottom sediments and determination of bathymetric changes show the potential for reworking of sediments, hence, areas vulnerable to contamination can be predicted.

Aside from validating depth-integrated circulation models, the results of this study also emphasize the different modes and pattern of transport between suspended and bottom sediment load that can be derived from Landsat images, grain size trends and bathymetric changes. Remotely-sensed data can complement in situ sampling and provide instantaneous lateral distribution and transport of suspended sediments. Sediment data, on the other hand, provide information on the long-term deposition and possible reworking of the sediments, while bathymetric changes reflect the total sediment transport scenario in the bay over a longer time span. Thus, it is necessary to combine the results to provide for the best estimates of how water and materials are transported throughout the coastal system. Future investigations will involve the use of high-resolution multi-beam echosounder for further validation of the results.

ACKNOWLEDGMENTS

This study was supported by grants from the National Institute of Geological Sciences-University of the Philippines at Diliman (UPD) and by the Office of the Vice Chancellor for Research and Development (UPD) under Grant No. 09817 NS. The Landsat data were provided by the Mines and Geosciences Bureau – Department of Environment and Natural Resources. John Ong wrote the computer program for the determination of sediment transport direction.

REFERENCES CITED

ASSELMAN NEM. 1999. Grain-size trends used to assess the effective discharge for floodplain sedimentation, River Waal, the Netherlands. J Sediment Res 69(1): 51–61.

BALSINHA M, FERNANDES C, OLIVEIRA A, RODRIGUES A, TABORDA R. 2014. Sediment transport patterns on the Estremadura Spur continental shelf: Insights from grain-size trend analysis. J Sea Res 93: 28–32.

BLUMBERG AF, SIGNELL RP, JENTER HL. 1993. Modeling transport processes in the coastal ocean. J Mar Environ Eng 1(1): 31–52.

CHENG P, GAO S, BOKUNIEWICZ H. 2004. Net sediment transport patterns over the Bohai Strait based on grain size trend analysis. Estuar Coast Shelf Sci 60: 203–212.

DE LAS ALAS JG, SODUSTA JA. 1985. A model for the wind driven circulation of Manila Bay. Nat App Sci Bull 37 (2): 159–170.

DOXARAN D, FROIDEFOND JM, CASTAING P, MARCEL BABIN M. 2009. Dynamics of the turbidity maximum zone in a macrotidal estuary (the Gironde, France): Observations from field and MODIS satellite data. Estuar Coast Shelf S 81(3): 321–332.

DUMAN M, AVCI M, DUMAN S, DEMIRKURT E, DUZBASTILAR MK. 2004. Surficial sediment distribution and net sediment transport pattern in I'zmir Bay, western Turkey. Cont Shelf Res 24: 965–981.

DYER KR. 1994. Estuarine sediment transport and deposition. In: Pye K, editor. Sediment Transport and Depositional Processes. Oxford: Blackwell Scientific Publications. p. 193–218.

FENG H, JIANG H, GAO W, WEINSTEIN MP, ZHANG Q, ZHANG W, YU L, YUAN D, TAO J. 2011. Metal contamination in sediments of the western Bohai Bay and adjacent estuaries, China. J Environ Manage 92(4): 1185–1197.

FINLEY RJ, BAUMGARDNER RWJR. 1980. Interpretation of surface-water circulation Aranasa, Texas, using Landsat imagery. Remote Sens Environ 10(3): 3–22.

FLEISCHER P, MCREE GJ, BRADY JJ. 1977. Beach dynamics and erosion control, Ocean View section, Norfolk, Virginia. Issue 30 of Technical Report 1977. Old Dominion University Institute of Oceanography. 185 p.

FOLK RL, WARD W. 1957. Brazos River bar: A study in significance of grain-size parameters. J Sed Petrol 27: 394–416.

FUJI-IE W, YANAGI T. 2006. Numerical experiment on sedimentation in Manila Bay. Coast Mar Sci 30(1): 54–61.

FUJI-IE W, YANAGI T, SIRINGAN FP. 2002. Tide, tidal current and sediment transport in Manila Bay. La Mer 40: 137–145.

GAO S, COLLINS M. 1992. Net sediment transport patterns inferred from grain-size trends, based upon definition of "transport vectors". Sediment Geol 80: 47–60.

GAO S, COLLINS M. 1994. Analysis of grain size trends for defining sediment transport pathways in marine environments. J Coast Res 210(1): 70–78.

GAO S, COLLINS MB, LANCKNEUS J, DE MOOR G, VAN LANCKNER V. 1994. Grain size trends in relation with net sediment transport patterns: An example from the Belgian continental shelf. Mar Geol 121: 171–185.

GOODRICH DM, BLUMBERG AF. 1991. The fortnightly mean circulation of Chesapeake Bay. Estuar Coast Shelf S 32: 451–462.

HORN DP, MASON T. 1994. Swash zone sediment transport modes. Mar Geol 120: 309–325.

JACINTO GS, SAN DIEGO-MCGLONE MLL, VELASQUEZ IB, SMITH SV. 1999. N and P budget of Manila Bay, Philippines. In: Watson I, Vigers G, Ong KS, McPherson C, Millson N, Tang A, Gass D, editors. Proceedings of the ASEAN Marine Environmental Management: Toward Sustainable Development and Integrated Management of the Marine Environment at the Fourth ASEAN-Canada Technical Conference on Marine Science; 1998 October 26–30; Langkawi, Malaysia. p. 341–345.

KAIRYTE M, STEVENS RL. 2015. Composite methodology for interpreting sediment transport pathways from spatial trends in grain size: A case study of the Lithuanian coast. Sedimentology 62: 681–696.

LAW BA, HILL PS, MILLIGAN TG, CURAN KJ, WIBERG PL, WHEATCROFT RA. 2008. Size sorting of fine-grained sediments during erosion: Results from the western Gulf of Lions. Cont Shelf Res 28 (2008): 1935–1946.

LE ROUX JP, O'BRIEN RD, RIOS F, CISTERNAS M. 2002. Analysis of sediment transport paths using grain-size parameters. Comput Geosci 28: 717–721.

LE ROUX JP, ROJAS EM. 2007. Sediment transport patterns determined from grain size parameters: Overview and state of the art. Sediment Geol 202: 473–488.

LEWIS DW, MCCONCHIE D. 1994. Analytical Sedimentology. New York: Chapman and Hall. 197 p.

MA F, WANG Y, LI Y, YE C, XU Z, ZHANG F. 2010. The application of geostatistics in grain size trend analysis: A case study of eastern Beibu Gulf. J Geog Sci 20(1): 77–90.

MACHADO W, SANTELLI RE, CARVALHO MFB, MOLISANI MM, BARRETO RC, D. LACERDA LD. 2008. Relation of reactive sulfides with organic carbon, iron, and manganese in anaerobic mangrove sediments: Implications for sediment suitability to trap trace metals. J Coast Res 24(4A): 25–32.

MAILLET GM, POIZOT E, SABATIER F, VELLA C, MEAR Y. 2011. Pattern of sediment transport in a microtidal river mouth using geostatistical sediment-trend analysis. J Sediment Res 81(2): 138–152.

MCLAREN P, LITTLE DI. 1987. The effects of sediment transport on contaminant dispersal: An example from Milford Haven. Mar Pollut Bull 18(11): 586–594.

MCLAREN P, HILL SH, BOWLES D. 2007. Deriving transport pathways in a sediment trend analysis (STA). Sediment Geol 202: 489–498.

PAVELSKY TM, SMITH LC. 2009. Remote sensing of suspended sediment concentration, flow velocity, and lake recharge in the Peace-Athabasca Delta, Canada. Water Resour Res 45(11): 1–16, W11417, doi:10.1029/2008WR007424.

POIZOT E, ANFUSO G, YANN M, BELLIDO C. 2013. Confirmation of beach accretion by grain-size trend analysis: Camposoto beach, Cadiz, SW Spain. Geo-Mar Lett 33: 263–272.

POKAVANICH T, NADAOKA K. 2006. Three-dimensional hydrodynamics simulation of Manila Bay. In: Proceedings of the Symposium on Infrastructure Development and the Environment; 2006 December 7–8; Diliman, Quezon City, Philippines: University of the Philippines. p. 1–14.

RAHARIMAHEFA T, KUSKY TM. 2010. Environmental monitoring of Bombetoka Bay and the Betsiboka Estuary, Madagascar, using multi-temporal satellite data. J Earth Sci 21(2): 210–226.

SANCHEZ A, CARRIQUIRY JD. 2011. Sediment transport patterns in Todos Santos Bay, Baja California, Mexico, inferred from grain-size trends. In: Manning AJ, editor. Sediment Transport in Aquatic Environments. Rijeka, Croatia: INTECH Open Access. p. 3–18.

SANTOS JR G, VILLAMATER DT. 1986. Dating of Manila Bay sediments. The Phil Geol 11(3): 21–31.

SINGER JK, ANDERSON JB. 1984. Use of total grain size distributions to define bed erosion and transport for poorly sorted sediment undergoing simulated bioturbation. Mar Geol 57: 335–359.

SIRINGAN FP, RINGOR CL. 1997. Predominant nearshore sediment dispersal patterns in Manila Bay. Science Diliman 9(1 & 2): 29–40.

SIRINGAN FP, RINGOR CL. 1998. Changes in bathymetry and their implications to sediment dispersal and rates of sedimentation in Manila Bay. Science Diliman 10(2):12–26.

STEVENS RL, BENGTSSON H, LEPLAND A. 1996. Textural provinces and transport interpretations with fine-grained sediments in the Skagerrak. J Sea Res 35(1-3): 99–110.

SUI SF. 1994. Waves in South China Sea. In: Zhou D, editor. Oceanology of China Seas Vol. 1. Netherlands: Kluwer Academic Publishers. p. 135–140.

THURMAN HV. 1988. Introductory Oceanography. 5th ed. Columbus, Ohio: Merrill Publishing Company. 515 p.

VELASQUEZ IB, JACINTO GS, VALERA FS. 2002. The speciation of dissolved copper, cadmium and zinc in Manila Bay, Philippines. Mar Pollut Bull 45: 210–217.

VILLANOY C, MARTIN M. 1997. Modeling the circulation of Manila Bay: Assessing the relative magnitudes of wind and tide forcing. Science Diliman 9(1 & 2): 41–52.

WISEMAN WJJR, SCHROEDER WW, DINNEL SP. 1988. Shelf-estuarine water exchanges between the Gulf of Mexico and Mobile Bay, Alabama. In: Weinstein MP, editor. Larval Fish and Shellfish Transport Through Inlets. American Fisheries Society Symposium 3. 1985 August 19–20; Ocean Springs, Mississippi, USA. p. 1–8.

ZHANG W, ZHENG J, XIAOMEI J, HOITINK AJF, VAN DER VEGT M, ZHU Y. 2013. Surficial sediment distribution and the associated net sediment transport pattern retain in the Pearl River Estuary, South China. Cont Shelf Res 61–62: 41–51.